Computational study of the interplay between intermolecular interactions and CO2 orientations in type I hydrates

Martín Pérez-Rodríguez, Ángel Vidal-Vidal, J. M. Míguez, Felipe Jiménez Blas, Jean-Philippe Torre, Manuel M. Piñeiro

Computational study of the interplay between intermolecular interactions and CO_2 orientations in type I hydrates

M. Pérez Rodríguez,[a] A. Vidal Vidal,[a] J. M. Míguez,[b] F. J. Blas,[b] J. P. Torré[c] and M. M. Piñeiro*[a]

Carbon dioxide (CO_2) molecules show a rich orientation landscape when they are enclathrated in type I hydrates. Previous studies have described experimentally their preferential orientations, and some theoretical works have explained, but only partially, these experimental results. In the present paper, we use classical molecular dynamics and electronic density functional theory to advance in the theoretical description of CO_2 orientations within type I hydrates. Our results are fully compatible with those previously reported, both theoretical and experimental, the geometric shape of the cavities in hydrate being, and therefore, the steric constraints, responsible for some (but not all) preferential angles. In addition, our calculations also show that guest guest interactions in neighbouring cages are a key factor to explain the remaining experimental angles. Besides the implication concerning equation of state hydrate modeling approximations, the conclusion is that these guest guest interactions should not be neglected, contrary to the usual practice.

DOI: 10.1039/c6cp07097c

1 Introduction

Hydrates are non-stoichiometric inclusion solids where water molecules form a crystalline regular network through hydrogen bonding, leaving cage structures that may enclathrate small guest molecules, such as carbon dioxide (CO_2).[1,2] Clathrate hydrates, also called gas hydrates, crystallize at low temperatures or moderately high pressures, but not so low temperatures or high pressures as usual for ice. Numerous research efforts from different scientific and technological communities have been devoted to study CO_2 gas hydrates, due to the applications and industrial processes where they are involved,[3–5] as for instance their potential to capture and store greenhouse effect gases,[6,7] especially CO_2 sequestration.[8,9] One very attractive idea, although not yet accessible in practice, is the exchange of CO_2 for the methane trapped inside naturally occurring hydrates in the ocean seabed and permafrost soils.[10,11] Komatsu *et al.*[12] have recently reviewed the experimental progress towards this CO_2–CH_4 replacement. This process would connect the potential future exploitation of hydrates as a methane source[13] with the long term storage of this greenhouse gas, meaning a high added-value environmental side effect. The feasibility of this application depends to a great extent on the detailed knowledge of the structural properties and dynamics of CO_2 molecules inside the hydrate, a key to guess the optimal replacement process.

Much effort has been devoted to the use of different molecular simulation tools to investigate microscopic features of hydrates and clathrates. English and MacElroy[14] have recently published a comprehensive review of the state-of-the-art in this field. Barnes and Koh[15] have also presented a more succinct review of the topic. Dynamic phenomena such as hydrate nucleation or growth comprise time and length scales hardly accessible through experimentation, and thus molecular simulations, with all its complementary approaches, has become an extremely useful tool to guess and propose molecular scale mechanisms to better understand hydrate science.

CO_2 produces the so-called type I hydrate structure, which is composed of two different cages. The first is a truncated hexagonal trapezohedron consisting of 12 pentagonal and 2 hexagonal faces (denoted hereafter as T cell for brevity, sometimes referred to in the literature as 5^{12} 6^2). The second cell type is a dodecahedron consisting of 12 pentagonal faces (D cell, or 5^{12}). Methane replacement by CO_2 entails processes of crystallization–dissociation, and also transport of guest molecules inside a permanent water lattice. In this context, during the simulation of the spectra of type I hydrates,[16] we faced an interesting problem: CO_2 being a linear

[a] *Dpto. de Física Aplicada, Fac. de Ciencias, Univ. de Vigo, E36310, Spain. E mail: mmpineiro@uvigo.es*

[b] *Laboratorio de Simulación Molecular y Química Computacional, CIQSO Centro de Investigación en Química Sostenible and Departamento de Física Aplicada, Facultad de Ciencias Experimentales, Universidad de Huelva, E21071 Huelva, Spain*

[c] *UMR 5150 Laboratoire des Fluides Complexes et leurs Réservoirs, Université de Pau et des Pays de l'Adour, B. P. 1155, Pau, Cedex 64013, France*

molecule, the transition barrier when passing from one cage to another depends to a great extent on its orientation. This implies that all the transport properties are also directly dependent on the preferred orientations, adding up to the guest–lattice interactions and other higher-order phenomena. This topic was studied previously by several groups using different approaches with not entirely clarifying results. The objective of this work is to discuss some aspects relative to the orientations of CO_2 molecules inside the type I hydrate, using standard computational tools, in order to improve the understanding about this aspect of the complex behavior of CO_2 hydrates.

It is worth noting that in this work, as in the previous ones,[16,17] we have used aperiodic hydrate cells to perform electronic density functional theory (DFT) calculations. The limitations of this cage only approach are evident (see *e.g.* the cited review of English and MacElroy[14] for a detailed discussion), due to the lack of periodic boundary conditions. Nevertheless, this technique has been widely used[18–23] due to the limitations imposed by the highly CPU demanding calculations involved. Bearing the limitations of this approach in mind, and knowing that fully periodic calculations of hydrates are becoming feasible (as demonstrated by English and Tse[24] or Hiratsuka *et al.*[25]), the cage only approach has proven useful and even quantitative in this context. In this work, *ab initio* calculations will be compared with classical molecular dynamics to discuss guest CO_2 preferred orientations.

2 Methods

Quantum calculations were performed using the density functional theory (DFT)[26] approach. In particular, B3LYP/6-311+g(d,p) was used for the angle series calculations. B3LYP stands for the Becke[27] three-parameter hybrid functional, which includes the Lee–Yang–Parr correlation.[28] This functional was chosen for two reasons. On one hand, considering the computational cost of the methods employed, there are a number of alternatives, especially the Truhlar family (M06, M08, *etc.*). However, they have been shown recently to be inferior to B3LYP for the simulation of the IR-visible spectra.[29] On the other hand, in previous works,[16,17] we have found that explicit long range correction methods such as CAM-B3LYP do not significantly improve the geometric results, and thus they were discarded due to their much higher computational demand. The above basis set was chosen bearing efficiency in mind, as it is the lowest level option possible that can deal with non-covalent interactions and H-bonds, which are of primary importance in the hydrate structures. One polarization function for each atom – p type for H atoms and d type for the other atoms – and an additional set of diffuse functions (+) for the non-H atoms were considered. Calculations were performed using Gaussian 09.[30] Two-cage systems were modelled at a lower level, B3LYP/6-31+g, due to the large number of atoms present.

Structures were built considering the lowest energy H-bond network. The number of possible conformations of a H-bond network of a T cage satisfying the Bernal–Fowler ice rules[31] is as large as 3 043 836, making it impossible in practice to consider all of them in energy calculations.[32] However, the difference between the lower energy conformation and the next immediately higher one is only about 2.5 kJ mol^{-1}. Therefore, only the lowest energy proton disorder conformations were used during the present work.

Geometric parameters were obtained using VMD[33] and pictures of the systems were rendered using included Tachyon ray-tracing utility.[34]

For molecular dynamics (MD) calculations, the unit cell of type I hydrate was built from the crystallographic coordinates available in the literature.[35] The initial CO_2 hydrate configuration was obtained by replicating this unit cell twice in each spatial direction ($2 \times 2 \times 2$), resulting in a total of 368 water molecules with 64 cavities. Hydrogen atoms were placed using the algorithm proposed by Buch *et al.*[36] to take into account the hydrate proton disorder, with the aim of generating solid configurations satisfying the Bernal–Fowler rules,[31] with zero (or at least negligible) dipole moment.

All molecular dynamics simulations were carried out in the isothermal–isobaric *NPT* ensemble using GROMACS (version 4.6.1).[37,38] Constant temperature (260 K) and pressure (40 MPa) were kept using a Nosé–Hoover[39,40] thermostat and a Parrinello–Rahman[41,42] barostat with a relaxation time of 2 ps. Under these conditions, the simulation box contained a single hydrate slab, as demonstrated in a previous work for the molecular models used,[43] and the guest occupancy considered was 100%, *i.e.* each cavity in the hydrate structure contained one guest CO_2 molecule. All three sides of the simulation box were allowed to fluctuate independently. The usual complete periodic boundary conditions and minimum image convention were followed. The time-step used was 2 fs, and the typical length of the runs varied between 80 ns and 400 ns. Intermolecular interactions were calculated as a sum of two contributions, Lennard-Jones (LJ) pairwise interactions, which were truncated at 9 Å, and electrostatic interactions, which dealt with the Ewald sums method. The real part of the Coulombic potential was truncated also at 9 Å and the Fourier term of the Ewald sums was evaluated using the particle mesh Ewald (PME) method.[44] The width of the mesh was 1 Å with a relative tolerance of 10^{-3} Å.

H_2O was modelled using the well-known rigid non-polarizable TIP4P[45] molecular geometry: four interacting centres, with the oxygen atom O as the only LJ interaction site, a point electric charge (M-site) located along the H–O–H angle bisector, and two hydrogen atoms H, which are represented by point electric charges. For CO_2, the most popular structure in the category of rigid non-polarizable models is a linear chain with three interacting sites, describing each C and O atoms as a combination of a LJ site plus an electric point charge. Among the available parametrizations for this structure, we have selected the TraPPE[46] version. The LJ H_2O–CO_2 interaction was calculated using the crossed interaction parameters given by the Lorentz–Berthelot combining rules.[47] The combination of these molecular models has been recently used to determine CO_2 hydrate three phase line equilibria[43,48] with remarkable quantitative accuracy. The choice of the optimal molecular force field to describe this type of

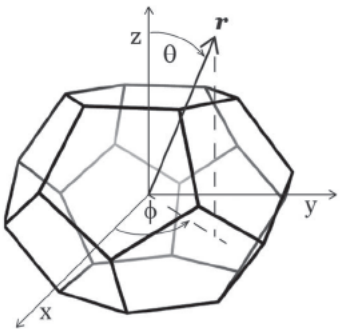

Fig. 1 T cell showing the reference Cartesian axes (x, y, z), and related orientation angles (θ, ϕ) of vector **r**. θ is the angle with respect to positive z, and ϕ is the angle with respect to the positive x in the (x, y) plane.

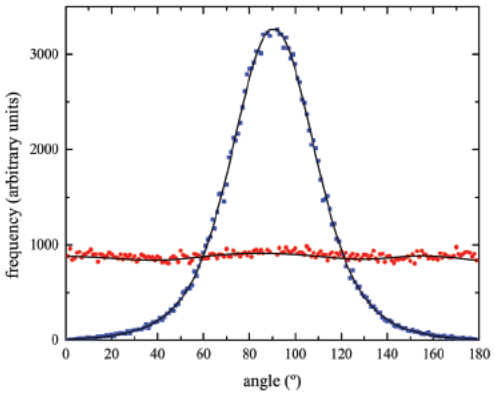

Fig. 2 Frequency plot of θ (blue squares) and ϕ (red circles) orientation angles of a CO_2 molecule inside a T cage, calculated from MD simulations.

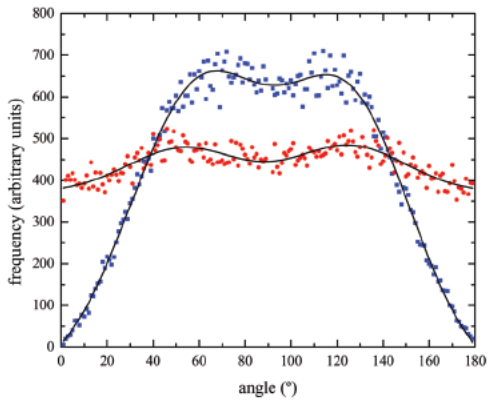

Fig. 3 Frequency of angles θ (blue squares) and ϕ (red circles) of a CO_2 molecule inside a D cage, as calculated by means of MD.

hydrates has been discussed previously for instance by English and Clarke[49] and Anderson *et al.*[50] They showed the enhanced ability of the CO_2 potentials adjusted to *ab initio* hydrate calculations. In this case, we have used well-known force fields that have been shown to perform accurately in the description of solid phases also in the case of CO_2.[51]

In Fig. 1, the Cartesian coordinates used in the following are depicted for a T cage. The axis perpendicular to both hexagonal faces corresponds to the z-coordinate, the hexagonal faces being parallel to the (x, y) plane. This will be the main framework of reference to analyze MD trajectories. For convenience, we will use spherical coordinates of the guest molecule to identify the different orientations. This way, the orientation will be described by two angles, θ, the angle with respect to +z, and ϕ, the angle with respect to the +x semi-axis on the (x, y) plane. For a D cage, the axes are not shown because the orientation is much simpler due to the symmetry. In this case the z-axis is chosen to be perpendicular to two opposite pentagonal faces. Due to the rotational symmetry of these D cells, results of different D cells will be comparable regardless of the faces selected as a reference of the z-axis placement. The analysis of guest molecule orientations within hydrate cells has been the object of previous studies. English and co-workers[24,52] used kubic harmonics to determine the preferential alignment of guest molecules.

3 Results and discussion

3.1 Molecular dynamics

Molecular dynamics of type I hydrate containing CO_2 were performed following the description given in Section 2. Snapshots of the system were taken along the production simulation runs, and, for each of them, the orientations of each guest molecule within the hydrate were determined and stored in a cumulative way. Distributions of probability for θ and ϕ angles inside a T cage are shown in Fig. 2. Three independent runs were carried out to check reproducibility, but only the results of the first run are shown, because those corresponding to the remaining two repetitions are fully compatible. The ϕ angle follows a uniform distribution while the θ profile corresponds to a normal distribution. In the D cage (Fig. 3), the distribution of θ is bimodal, with two small and rather flat peaks around $\pm 25°$ with respect to the equatorial plane (x, y). For ϕ, the profile deviates only slightly from a uniform distribution, being also bimodal, around $\theta = 90 \pm 30°$.

Therefore, the molecular conformation in T cages is clearly equatorial, with complete rotational freedom along ϕ angle, whereas in D cages the most favorable orientations are deviated about $\pm 30°$ with respect to the equatorial plane. If we consider a D cage as an ideal regular dodecahedron, and the normal from the center of the faces, we find that, given one of them, the other possible normal orientations are distributed in two layers at the approximate values found for θ. The bimodal shape of ϕ is less relevant, probably due to deviation of the D cage from the ideal regular polyhedron that effectively occurs in type I hydrate. In the case of D, it is also noteworthy that the count ratio θ/ϕ at peak values is much lower than that in T, so the preferential orientations are not so populated in the case of D, indicating a more regular distribution.

Fig. 4 represents the power spectrum of each atom type in H_2O and CO_2 molecules separately, obtained by the analysis of the MD trajectory. The power spectrum is the Fourier transform of the molecular velocity autocorrelation functions (VACFs). This spectrum is quite similar, in what concerns to host molecules, to those obtained by Tse *et al.*[53] for several types of guest molecules for type I hydrate. It must be taken into

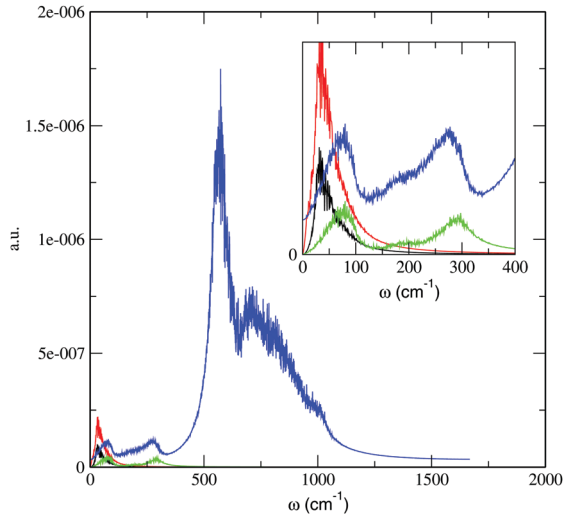

Fig. 4 Power spectra of H atom (blue line) and O atom (green line) in a H_2O molecule, and C atom (black line) and O atom (red line) in a CO_2 molecule, obtained from MD trajectory. The inset magnifies the lower frequency range.

account that these VACFs were calculated from a classical MD simulation, performed considering rigid molecular models for both H_2O and CO_2. Thus, internal atomic vibrations are not sampled at all, and Fig. 4 represents the purely translational density of states, depending on kinetic and potential energies only. This figure shows a certain overlapping between the bands of O atoms of both molecules. In order to guess the relative intensity of the host and guest intermolecular interaction energies, these values have been computed also from a classical MD run, separating the Lennard-Jones and Coulombic contributions, listed in Table 1. These values show that host–guest interactions are quite weak, and mostly of dispersive nature.

These results obtained for the CO_2 preferential orientations within the hydrate are compatible with other ones reported previously in the literature, either obtained from MD calculations[54] or experimentally.[55] However, some particular values of these preferred orientation angles determined experimentally at low temperatures are not reproduced with the calculations presented so far. For this reason, an additional DFT approach was also considered here, in order to obtain a more detailed individual cage geometric description.

3.2 DFT: individual cages

The most simple and computationally accessible hydrate model from the DFT perspective is the isolated cage. Despite the cited limitations for this approach, which must be always kept in mind,

Table 1 Intermolecular potential energy determined using classical MD (all values in kJ mol^{-1}). Errors were determined in each case by block averaging

Interaction	H_2O H_2O	CO_2 H_2O	CO_2 CO_2
L J	5236 ± 2	-1309 ± 1	-67.01 ± 0.05
Coulombic	-27043 ± 3	-315.5 ± 0.5	-58.3 ± 0.1

type I hydrate properties can be described to a great extent by calculating separately the corresponding properties of isolated T and D cages. This applies for instance to infrared and Raman spectra,[16] and therefore, this approach will be used here as well as first approximation.

The effects of network periodicity and system size might be explored if the same DFT calculations were performed on a hydrate cell verifying periodic boundary conditions as in MD. The problem is that this calculation entails a large number of molecules, and the preliminary attempts we performed to test this option did not yield satisfactory results. Another option is to use the same periodic box to perform *ab initio* molecular dynamics. This test has been also performed in this case, using the Born–Oppenheimer approximation (BOMD). The trajectory step size used was 0.25 $(amu)^{1/2} \times$ Bohr and the integration step was 0.2 fs. We performed 100 steps resulting in approximately 30 fs of total simulation time. Therefore, only wavelengths below 15 fs can be adequately estimated. Nevertheless, the trend of the molecular axis orientation evolution allows us to guess lower bounds for the CO_2 molecular rotation period by extrapolation. In a previous work[16] we compared CO_2 experimental Raman spectra with the calculations obtained using the same setup used here. The anti-symmetric stretching vibration, denoted usually as ν_3, lies at approximately 2420 cm^{-1}, which corresponds to a period value of 13.78 fs. This is the vibration that is accessible in the time range we evaluated in our calculations. If we consider the symmetric stretching, ν_1 with 1347 cm^{-1} (24.76 fs), or the two bending bands $\nu_{2a,b}$ at around 678 cm^{-1} (49.19 fs), we can realize that their periods are too large to be sampled in the calculations we have performed. Additionally, molecular rotations are in the scale of picoseconds. This estimation is necessary to ensure that the time step considered in the MD simulations is consistent to provide a statistically sound sampling of the orientations.

3.2.1 T type cage. A series of 180° intervals for the θ angle, in steps of 2°, were considered for three complementary cases, each of them corresponding to a trajectory where the ϕ angle is fixed: one trajectory passing in front of the oxygen (of a hexagonal face), another one passing near the closest H, and the third one passing in front of the more distant H atom. The three cases serve to describe the whole T cell, due to its 6-fold symmetry, and are illustrated in Fig. 5. To avoid local effects, the different orientations were chosen to be non-adjacent on purpose. Using this simple strategy, the global energy minimum and maximum are expected to be reached, without the need of a more exhaustive sampling, and due to that fact, the point density in each series can be higher within a reasonable total computing time.

The obtained profiles are smooth but slightly irregular due to the asymmetry of the calculated T structure. This is an expected consequence of optimizing the geometry of an isolated cell by means of DFT. We have observed that isolated cells tend to distort to a triangular prism shape, whereas a cell inside the crystal tends to distort to a square prism. This effect is very subtle, but noteworthy, because it is indicative of some limitations of considering only isolated cells or small clusters in describing the

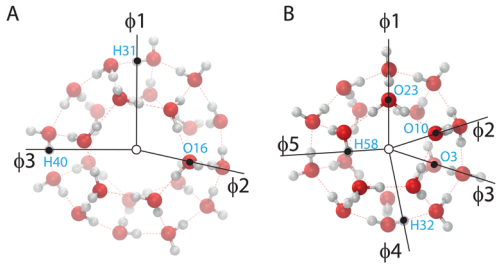

Fig. 5 (A) T cage viewed along the z axis ((x, y) plane is parallel to the paper), showing the different orientations in ϕ angle chosen for calculating θ series. The atoms that were used as a reference for the orientations are marked with a blue label and a black dot. (B) An equivalent representation of D cage.

average cell structure. Nevertheless, other approximations made in this work, especially the choice of the minimum energy structure while being far from zero temperature, will probably have more significant effects on the general results.

Differences of SCF energy profiles are represented in Fig. 6. The global minimum was used as the reference for all the energy series, but differences between minima are almost negligible. The most probable configuration found in all cases is that of the CO_2 molecular axis being parallel to the (x, y) plane, in good agreement with our previous MD calculations and also with the literature results.[54] Nevertheless, only in the ϕ^3 case (see Fig. 5A) the most favourable orientation is actually $\theta = 90^\circ$. In the other two cases, the minimum angle is deviated about 5° from the (x, y) plane. This deviation is compatible with

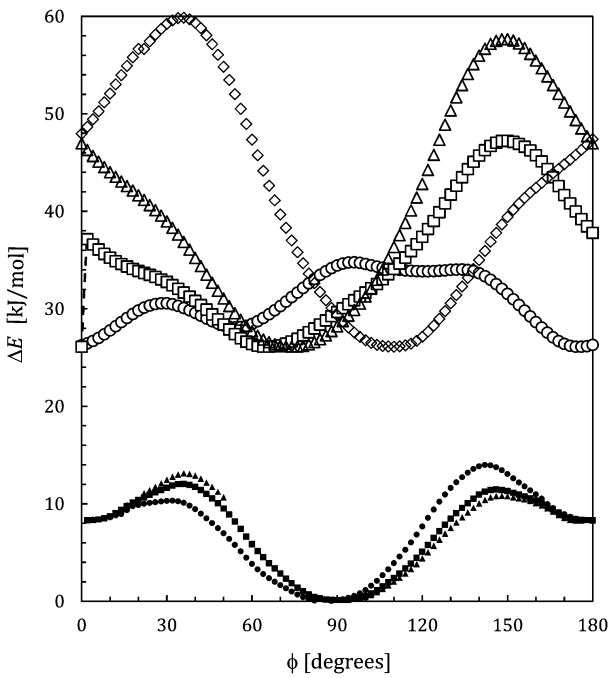

Fig. 6 Energy profiles of D (hollow markers) and T (solid markers) cells containing one CO_2 molecule, as a function of the angle θ. Several ϕ orientations are represented for each cell, passing in front of different steric interaction regions, as illustrated in Fig. 5. Markers are as follows: for D cell, circles, $\phi 1_D$; squares, $\phi 2_D$; diamonds, $\phi 3_D$; and triangles, $\phi 5_D$; for T cell, circles, $\phi 1_T$; squares, $\phi 2_T$ and triangles, $\phi 3_T$.

the low temperature MD calculations by Alavi *et al.*,[54] and also with the experimental results reported by Udachin *et al.*[55] A plausible cause for these small deviations is the van der Waals interaction between the guest molecule and the water lattice, considering that CO_2 does not occupy all accessible space inside the T cell. This hypothesis is supported by the fact that the path for which the minimum is $\theta = 0^\circ$ is the less populated one of the three considered. A secondary minimum is observed in the orientation parallel to the z-axis, with an energy depth of about one-third of the primary one. The associated probability is, therefore, much lower, but the conformation was also found to be stable.

3.2.2 D type cage. A similar procedure was used for the study of D cage orientations. Again, several θ series at selected ϕ orientations were calculated. Five representative cases of different ϕ values are shown in Fig. 6. The results are in general in good agreement with the experimental data of Udachin *et al.*[55], although the differences with respect to the ideal orientation due to the geometry are lower in our calculations. They reported that in D cages the preferential orientations of CO_2 fall between 15° and 20° from the axis perpendicular to a pair of opposite pentagonal faces. Starting from a similar orientation in the z-direction (and after a geometric optimization), two series of θ angle were calculated going through two different vertices of the upper face (hollow circles and squares in Fig. 6), and we found a discrepancy of -8° and $+8^\circ$ respectively when compared with the expected values of 180° and 60°. Two additional series passing in front of two vertices of the lower face (hollow rhombi and triangles) were calculated, the differences being -14° and 14° with respect to 120° and 60°.

If we compare T and D cages, the accessible volume inside the latter is smaller, which causes a higher value for the minimum energy inside D, and also the symmetry of the D cell is much closer to spherical, the minima and maxima being more evenly distributed over the orientation space (θ, ϕ). The D minima are apparent, as in the case of T, but now the variation values span over a broader interval than in the case of T, due to greater steric constraints. The difference in the global geometric minimum between CO_2@T and CO_2@D was calculated using a two-cage system TD, which will be described in the next sections, and minimizing the system with only one CO_2 molecule in either T or D cage. Its value was found to be 0.23 eV, and therefore a series for D cages (hollow markers) is shifted in that amount with respect to T values (solid markers) as shown in Fig. 6.

Udachin *et al.*[55] found two preferential deviations from the (x, y) plane in T cells: 6.4° and 14.4°. So far, our computed values are compatible only with the first value, but there are no clues about the second one. At this point, our principal hypotheses are two: on one hand, it is possible that a number of Bjerrum defects in the lattice promote H-bond interactions with the guest, forcing frequent alternative orientations not modeled in ideal cages. On the other hand, it is possible that neighbouring cells, not considered to this point, have a significant influence on the guest orientations. Due to relative rotational freedom of CO_2, we opted to explore this last possibility, and thus it will be discussed in the following sections.

3.3 DFT: two-cage systems

Systems consisting of two cages were then considered in order to evaluate the influence of neighbouring cages, in particular, the CO_2–CO_2 inter-cage couplings and their relative magnitudes. Interactions of first-neighbours of CO_2 inside the hydrate are usually neglected in EoS hydrate modelling approaches, as for instance in the widely used van der Waals–Platteeuw (vdWP) theory,[56,57] but as we will see in the following, they must be taken into account at the cell scale. The modification of EoS that this fact might imply for the calculation of thermodynamic properties is case-dependent and will not be discussed in depth in the present study. Couplings further away than the first-neighbours are also expected to occur, especially through the channels formed by the parallel hexagonal faces of consecutive T cages, but this is a statistical mechanics problem beyond the objectives of this work.

3.3.1 TT system. First, a system consisting of two identical T cells aligned in the *z*-direction was built up in the lower energy conformation of H-bond ordering. This double cell system, called TT, was optimized without guest molecules, and then re-optimized with one molecule of CO_2 inside each of them (Fig. 7). Several orientations representative of combinations of the minima found in isolated T cells were selected as starting structures. In the following, label 1 will represent the orientation of CO_2 along the *z*-axis, and label 2 will be perpendicular to this, *i.e.* parallel to the (x, y) plane. Finally, three main conformations were calculated, corresponding to the minimum energy in isolated cells, and were labeled accordingly: T_1T_1, T_2T_1 (equivalent to T_1T_2) and T_2T_2.

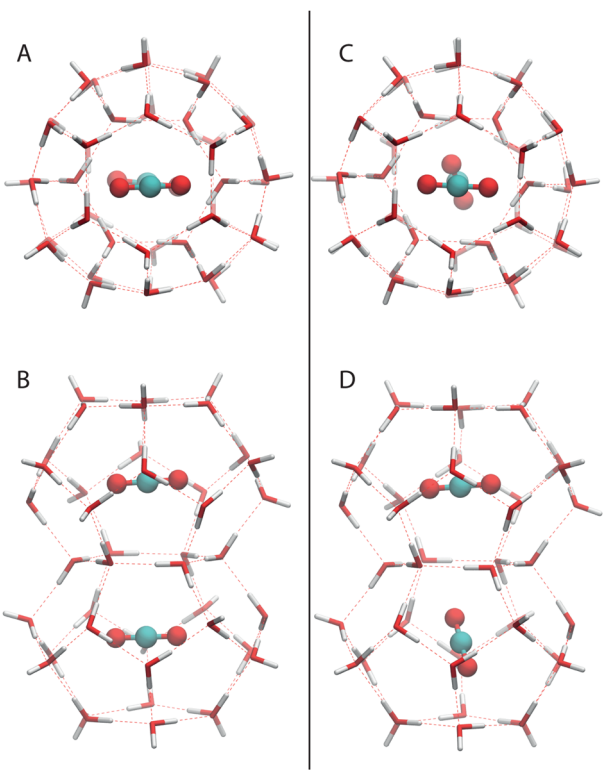

Fig. 7 Stable geometries of two cage TT system occupied by CO_2 guest molecules. (A) Top view of global minimum energy structure (T_2T_2) and (B) side view. (C) Top view of secondary minimum (local) energy structure (T_2T_1) and (D) side view.

Two of these conformations were found to be stable: T_2T_1 and T_2T_2, not surprisingly, T_2T_2 being the most favourable one (Fig. 7A and B). T_2T_1 follows very closely in energy with only $\sim$4 kJ mol^{-1} above the previous one (Fig. 7C and D). This difference becomes negligible when considering the thermal energy at the range of temperatures where hydrates are found in nature. T_1T_1 is completely unstable, contrary to the results obtained for one isolated T cell. For this initial configuration, the final (geometrically optimal) conformation is T_2T_2, as a result of a rotation of both CO_2 molecules, the corresponding energy and geometry being equivalent to the first case tested. These results demonstrate the inter-cage orientational coupling of CO_2 molecules and, moreover, strongly suggest that the coupling is direct and not mediated by the network of water molecules. The T_1T_1 optimization process supports this affirmation because it progresses with both CO_2 molecules, axes being parallel during a rotation of 90°, but at the same time, there is no apparent distortion in the water lattice during the rotation process.

The orientation in T_2T_2 conformation is compatible with the main results described before, θ angles being almost parallel to the equatorial plane but slightly deviated, between 0° and 4°. The relative ϕ angle between CO_2 molecules is also very small, about 8°. The T_2T_1 conformation results are more interesting because they introduce new orientations not obtained in the precedent isolated cell section. Deviation from the equatorial plane is $\sim$5° in T_2, compatible with the previous results for an individual T cell, but in T_1 it is approximately 51° (θ = 39°). Although this is not in the *z*-axis direction, the resultant relative orientation between CO_2 molecules resembles clearly a tee shape, with the vertical molecule oriented towards a position between C and O atoms in the horizontal molecule, and its oxygen atoms out of the plane. The relative dihedral angle between CO_2 molecules is approximately 70°, much more pronounced than that in T_2T_2. Distances between pairs of equivalent atoms in CO_2, starting with the nearest oxygen atoms, are O_2^{α}–O_1^{α} = 510 pm, O_2^{α}–C_1 = 511 pm, C_2–C_1 = 596 pm, O_2^{β}–O_1^{β} = 703 pm.

The C atom in the T_1 cell is, in both conformations, centered with respect to the cell geometry, making feasible a sequence of alternate 1 and 2 conformations along hexagonal T channels, $[T_2T_1T_2T_1T_2\ldots]$, besides the all-parallel sequence $[T_2T_2T_2\ldots]$. Therefore, any combination of both sequences seems feasible, provided that no pair of T_1T_1 appears, as for example: $[T_2T_2T_1T_2T_2T_2T_1T_2\ldots]$.

3.3.2 TD system. Another possibility for two guests in adjacent cells is to be in T and D cells respectively. This case was also calculated, and some additional comments are pertinent before discussing the results: a TD system is cell-asymmetric, so T_2D_1 has to be considered in addition to T_1D_2. Due to the D cell symmetry, only two conformations were chosen for D. Label 1 for a D cell in TD systems means that CO_2 is oriented toward the face adjacent to the hexagonal face of a T cell, *i.e.* the face which continues the surface of the hexagonal one on the T cell (see Fig. 8). Label 2 corresponds to the orientation towards the face

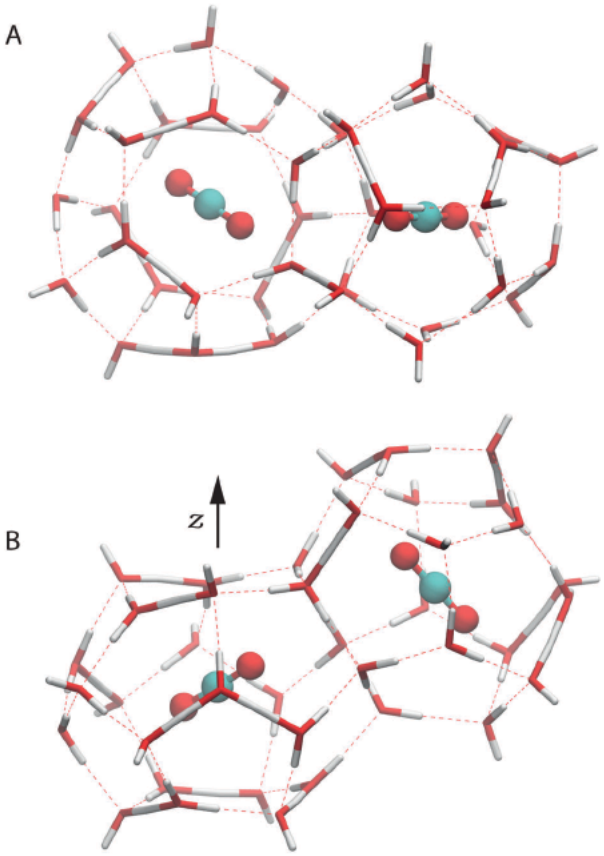

Fig. 8 Minimum energy geometry of two cage TD system containing two CO_2 guest molecules, corresponding to the T_2D_1 starting conformation. (A) Top view. (B) Side view.

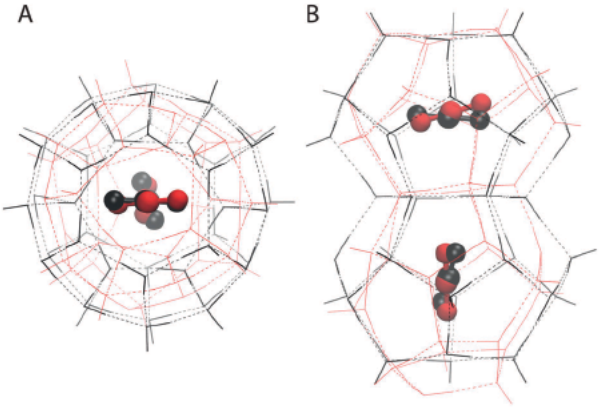

Fig. 9 T_2D_1 structure, in red, superimposed over T_2T_1, in black, illustrating the equivalence of both systems in terms of relative disposition of guests, (A) top view; (B) side view. Structures were aligned by means of pair fitting between corresponding atom positions of CO_2 molecules.

shared by T and D cells. So, D_1 is the orientation closer to the parallel axis of T_1, (to the *z*-axis of T cell also) and D_2 the closer to perpendicular. Actually, there is only one relative disposition of one D cell to an adjacent T cell, which is repeated around the equator of the T cells. We have chosen *z* as the reference axis, as in the precedent cases, and the four starting conformations T_1D_1, T_1D_2, T_2D_1, and T_2D_2.

Only one conformation was found to be stable, corresponding to the T_2D_1 orientation, and will be identified by that label. In this case, CO_2@T presents a deviation from the equatorial plane of about 19°, which is compatible with 14° of the secondary experimental result of Udachin *et al.*,[55] whereas CO_2@D is oriented at 14° with respect to the nearest axis connecting two opposite faces, in very good agreement with previously described results in D cages.

The T_2D_1 system is comparable to T_2T_1 in terms of relative CO_2–CO_2 orientations: the relative dihedral angle between CO_2 molecules is approximately 80° and distances between pairs of equivalent atoms in CO_2 are O_2^{α}–O_1^{α} = 499 pm, O_2^{α}–C_1 = 526 pm, C_2–C_1 = 631 pm, O_2^{β}–O_1^{β} = 783 pm. Dihedral angles differ only in 10°, distances O_2^{α}–O_1^{α} in 1 pm and C_2–C_1 in 16 pm. These values imply that T_2T_1 and T_2D_1 are in fact equivalent conformations from the point of view of relative disposition of guests, which implies that the interaction between them is of the same type. It was expected that interaction energies were lower in the TD system, due to smaller volume in the D cell, and the worse relative orientation of a water network with respect to the pair of guests. The equivalence is clearly illustrated when superimposing both structures, as in Fig. 9, where the coincidence in the guest positions is remarkably better than in the surrounding network of water molecules.

The obtained coupled conformations of CO_2 molecules are equivalent in T_2T_2 and T_2D_1 systems, and, therefore, they are expected to be also equivalent in TT systems connected through pentagonal faces. The reasons supporting this assumption are the symmetry of the location of pentagonal faces in T cells and the rotation freedom shown for the ϕ angle.

3.4 Guest–guest interactions

Once established the CO_2–CO_2 interaction between adjacent cages for TT and TD systems independently, there are questions that arise from the comparison of the results, and other details that were not previously commented, that deserve some attention in order to better understand the coupling. These will be discussed in the following.

One of the usual assumptions made when modelling hydrates is that there is no dipolar coupling between guest molecules and the water lattice, as for example in the analysis method for NMR signal anisotropy developed by Alavi *et al.*[54] The results we have found so far support this assumption and confirm that the interactions with the lattice are mainly dispersive. This holds if all H-bonds are involved in the water network, because otherwise some kind of interaction with C–O polar bonds of CO_2 might be expected. On the other hand, the interaction between guests seems to be caused by polar effects, because of the large distance between molecules, the hardly noticeable distortion of the lattice, and the stable relative orientations of guests. Quadrupole moments of CO_2 are arguably the main factor in T_2T_1 and T_2D_1 systems, as supported, for example, by the tee shaped relative orientations obtained in the phase equilibrium of solid CO_2 by Monte Carlo.[51] Steric constraints caused by the cage shape are more important in the T_2T_2 conformation than in T_2T_1 because

molecular charges are more effectively screened by the water molecules of the central hexagonal ring when both guests are in the equatorial plane, and they are farther away also, weakening the (multi)polar interactions. In T_2T_2, the resultant charge interaction is attractive, whereas in T_2T_1 and T_2D_1 it is repulsive, because equivalent partial charges in both guests are confronted, also having a significant contribution to the stabilization in the parallel conformation.

A careful observation of the T_1T_1 optimization process, where both CO_2 molecules rotate towards the T_2T_2 conformation, reveals a transition state at about 60 degrees from the *z*-axis. Simulations were repeated using different basis sets, obtaining consistently the same result. This particular orientation corresponds to a relative disposition where both guests have one of their bond dipoles C–O coupled with the other in parallel and with opposite directions: the most favorable geometry under vacuum of two CO_2 molecules. The other $CO_2 \cdots CO_2$ stable geometry is a tee shape equivalent to T_2D_1, but with all of the atoms lying in the same plane. On one hand, this observation further supports the quadrupole guest–guest interaction as the main factor behind the θ behavior. On the other hand, it also implies that ϕ is not conditioned by the guest–guest interaction, and depends mainly on the guest–host one. Under our suppositions, the latter is mostly of dispersive nature.

Summarizing the orientational results, in terms of the equatorial deviation in θ, we obtain that conformation T_2T_2 is characterized by angles $<10^\circ$ (6°); T_2T_1 by angles $>40^\circ$ (51°) and T2D1 with intermediate values, around 20° (19°). This last angle is in fact an overestimation of the real value, because of the simplification made considering only two cages. If we take into account all the possible first neighbors of a T cage, there are 2 hexagonal contacts with adjacent T cages, N(T6T) = 2, 8 pentagonal contacts with T cages, N(T5T) = 8, and 4 pentagonal contacts with D cages N(T5D) = 4. Assuming that the tee shaped stable conformation of T5T is equivalent to that of T5D, guest–guest interactions around equatorial discs of pentagons will not change the θ value in T cages. Nevertheless, interactions in the perpendicular *z*-axis will do, and the values of the angle close to the (x, y) plane being, they will be repulsive, tending to reduce the deviation value below the calculated 19°. T_2T_1 being a secondary minimum, it is not expected to have a significant probability in the angle distribution, as commented before, and we can therefore neglect its contribution to experimental results. The correspondence between θ angles and types of neighbouring cages suggest the theoretical possibility of determining the relative number of the two CO_2–CO_2 couplings by looking at the experimental angle distribution, and from it, the relative occupancy of T and D cages.

4 Conclusions

Orientations of CO_2 guest molecules inside cavities of type I hydrates were studied by means of MD and DFT approximations. MD bulk calculations and DFT performed in isolated D and T cages show a good agreement with the previous MD[54] and experimental[55] results found in the literature. Angle deviations of energy minima with respect to geometrically expected ones are of the same order of the previously reported ones.

Interactions between neighbours were studied in explicit two-cage TT and TD systems by means of DFT, with the aim of evaluating their relationship with guest orientations and to explain some additional experimentally observed angles.

Calculations have shown that CO_2 molecules in adjacent cells interact with each other. In particular, in TT systems, two stable conformations were found: (1) the most favorable was the one where both guests are aligned parallel and perpendicular to the *z*-axis, and (2) a secondary minimum where guests are organized in an approximated tee shape. The energy difference between them is only about 4 kJ mol^{-1}.

The optimization processes in TT show synchronous rotations of both guests when starting from an unstable geometry, supporting the hypothesis of a direct coupling between them.

Angles in the parallel conformation are compatible with the MD and DFT single cell calculations. An additional deviation of 51° from the equatorial plane was found in the DFT tee shaped conformation, but being a secondary minimum, it is expected to be negligible under experimental conditions and might not be detected.

Guest–guest coupling in the TD system was also observed, presenting only one stable conformation. Angles in the D cage for this conformation are in very good agreement with the DFT calculations in isolated cages. Angles in the T cage, about 19°, are compatible with the experimental ones of 14° with respect to the equatorial plane.

The TD minimum structure was found to be equivalent to the tee shaped secondary minimum of the TT system. This result, combined with the geometry of the T and D cells, suggests that the two described conformations, parallel and tee shape, are the only stable classes of CO_2 relative orientations in type I hydrates.

Guest–guest coupling is probably due to CO_2 quadrupole; the parallel conformation is stabilized because the repulsion of quadrupoles is increased if orientations are displaced from this equilibrium position, while in the tee conformation the interaction becomes attractive approaching guests against the steric constraints imposed by the cages. It is noteworthy that guest CO_2 mutual interactions have been pointed out to be relevant in the description of other clathrate systems, even using macroscopic thermodynamic models, as pointed out recently by Conde *et al.*[58]

A more detailed analysis shows that the two orientational coordinates are not fully coupled and, therefore, it suggests that they depend either on the guest–host interaction (ϕ) or on the guest–guest interaction (θ). This hypothesis would need further studies to be confirmed, but it could open a door to the experimental study of the guest–guest interactions and the cage occupancy *via* orientation profile measurements.

Acknowledgements

The authors acknowledge Centro de Supercomputación de Galicia (CESGA, Santiago de Compostela, Spain) for providing access to computing facilities, and Ministerio de Economía y Competitividad (MINECO, Spain) for financial support (FIS2013-46920-C2-1-P and FIS2015-68910-P). The authors also acknowledge

MCIA (Mésocentre de Calcul Intensif Aquitain) of the Universités de Bordeaux and Pau et Pays de l'Adour, France, for the computer resources provided for this work (JMM) and Carnot Institute ISIFoR (France) through the THEMYS project (JMM, JPT).

References

1 E. D. Sloan and C. Koh, *Clathrate Hydrates of Natural Gases*, CRC Press, New York, 3rd edn, 2008.
2 E. D. Sloan, *Nature*, 2003, **426**, 353–359.
3 A. K. Sum, C. A. Koh and E. D. Sloan, *Ind. Eng. Chem. Res.*, 2009, **48**, 7457–7465.
4 K. M. Sabil, N. Azmi and H. Mukhtar, *J. Appl. Sci.*, 2011, **11**, 3534–3540.
5 L. Fournaison, A. Delahaye, I. Chatti and J.-P. Petitet, *Ind. Eng. Chem. Res.*, 2004, **43**(20), 6521–6526.
6 C.-G. Xuab and X.-S. Li, *RSC Adv.*, 2014, **4**, 18301–18316.
7 P. Babu, P. Linga, R. Kumar and P. Englezos, *Energy*, 2015, **85**(1), 261–279.
8 K. Shin, Y. Park, M. Cha, K.-P. Park, D.-G. Huh, J. Lee, S.-J. Kim and H. Lee, *Energy Fuels*, 2008, **22**, 3160–3163.
9 G. Ersland, J. Husebo, A. Graue and B. Kvamme, *Energy Procedia*, 2009, **1**, 3477–3484.
10 *Natural Gas Hydrate in Oceanic and Permafrost Environments*, ed. M. D. Max, Springer, 2011.
11 M. D. Max, A. H. Johnson and W. P. Dillon, *Economic Geology of Natural Gas Hydrate*, Springer, 2006.
12 H. Komatsu, M. Ota, R. L. Smith and H. Inomata, *J. Taiwan Inst. Chem. Eng.*, 2013, **44**, 517–537.
13 R. Boswell and T. S. Collett, *Energy Environ. Sci.*, 2011, **4**, 1206–1215.
14 N. J. English and J. M. D. MacElroy, *Chem. Eng. Sci.*, 2015, **121**, 133–156.
15 B. C. Barnes and A. K. Sum, *Curr. Opin. Chem. Eng.*, 2013, **2**, 184–190.
16 A. Vidal-Vidal, M. Pérez-Rodríguez, J.-P. Torré and M. M. Piñeiro, *Phys. Chem. Chem. Phys.*, 2015, **17**, 6963–6975.
17 A. Vidal-Vidal, M. Pérez-Rodríguez and M. M. Piñeiro, *RSC Adv.*, 2016, **6**, 1966–1972.
18 C. Jameson and D. Stueber, *J. Chem. Phys.*, 2004, **120**, 10200–10214.
19 S. Alavi, J. Ripmeester and D. Klug, *J. Chem. Phys.*, 2006, **124**, 014704.
20 H. Conrad, F. Lehmkühler, C. Sternemann, A. Sakko, D. Paschek, L. Simonelli, S. Huotari, O. Feroughi, M. Tolan and K. Hämäläinen, *Phys. Rev. Lett.*, 2009, **103**, 218301.
21 P. Chattaraj, S. Bandaru and S. Mondal, *J. Phys. Chem. A*, 2011, **115**, 187–193.
22 K. Ramya and A. Venkatnathan, *J. Phys. Chem. A*, 2012, **116**, 7742–7745.
23 K. Ramya and A. Venkatnathan, *Indian J. Chem., Sect. A: Inorg., Bio-inorg., Phys., Theor. Anal. Chem.*, 2013, **52**, 1061–1065.
24 N. J. English and J. S. Tse, *J. Phys. Chem. A*, 2011, **115**, 6226–6232.
25 M. Hiratsuka, R. Ohmura, A. K. Sum and K. Yasuoka, *J. Chem. Phys.*, 2012, **136**, 044508.
26 W. Kohn and L. J. Sham, *Phys. Rev.*, 1965, **140**, A1133.
27 A. D. Becke, *J. Chem. Phys.*, 1993, **98**, 5648–5652.
28 C. Lee, W. Yang and R. G. Parr, *Phys. Rev. B: Condens. Matter Mater. Phys.*, 1988, **37**, 785.
29 *Computational Strategies for Spectroscopy*, ed. V. Barone, John Willey and Sons Inc., New Jersey, 2012.
30 M. J. Frisch, G. W. Trucks, H. B. Schlegel, G. E. Scuseria, M. A. Robb, J. R. Cheeseman, G. Scalmani, V. Barone, B. Mennucci, G. A. Petersson, H. Nakatsuji, M. Caricato, X. Li, H. P. Hratchian, A. F. Izmaylov, J. Bloino, G. Zheng, J. L. Sonnenberg, M. Hada, M. Ehara, K. Toyota, R. Fukuda, J. Hasegawa, M. Ishida, T. Nakajima, Y. Honda, O. Kitao, H. Nakai, T. Vreven, J. A. Montgomery Jr, J. E. Peralta, F. Ogliaro, M. Bearpark, J. J. Heyd, E. Brothers, K. N. Kudin, V. N. Staroverov, R. Kobayashi, J. Normand, K. Raghavachari, A. Rendell, J. C. Burant, S. S. Iyengar, J. Tomasi, M. Cossi, N. Rega, J. M. Millam, M. Klene, J. E. Knox, J. B. Cross, V. Bakken, C. Adamo, J. Jaramillo, R. Gomperts, R. E. Stratmann, O. Yazyev, A. J. Austin, R. Cammi, C. Pomelli, J. W. Ochterski, R. L. Martin, K. Morokuma, V. G. Zakrzewski, G. A. Voth, P. Salvador, J. J. Dannenberg, S. Dapprich, A. D. Daniels, Ö. Farkas, J. B. Foresman, J. V. Ortiz, J. Cioslowski and D. J. Fox, *Gaussian 09 Revision D.01*, Gaussian Inc., Wallingford CT, 2009.
31 J. D. Bernal and R. H. Fowler, *J. Chem. Phys.*, 1933, **1**, 515.
32 S. Yoo, M. V. Kirov and S. S. Xantheas, *J. Am. Chem. Soc.*, 2009, **131**, 7564–7566.
33 W. Humphrey, A. Dalke and K. Schulten, *J. Mol. Graphics*, 1996, **14**, 33–38.
34 J. Stone, MSc thesis, Computer Science Department, University of Missouri-Rolla, 1998.
35 M. Yousuf, S. B. Qadri, D. L. Knies, K. S. Grabowski, R. B. Coffin and J. W. Pohlman, *Appl. Phys. A: Mater. Sci. Process.*, 2004, **78**, 925–939.
36 V. Buch, P. Sandler and J. Sadlej, *J. Phys. Chem. B*, 1998, **102**, 8641.
37 A. Bekker, H. C. J. Brendsen, E. J. Dijkstra, S. Achterop, R. van Drunen, D. van der Spoel, A. Sijbers, H. Keegstra, B. Reitsma and M. K. R. Renardus, *Physics computing 92*, World Scientific, Singapore, 1993.
38 D. V. D. Spoel, E. Lindahl, B. Hess, G. Groenhof, A. E. Mark and H. J. C. Berendsen, *J. Comput. Chem.*, 2005, **26**, 1701.
39 S. Nosé, *J. Chem. Phys.*, 1984, **81**, 511.
40 W. G. Hoover, *Phys. Rev. A: At., Mol., Opt. Phys.*, 1985, **31**, 1695.
41 M. Parrinello and A. Rahman, *J. Appl. Phys.*, 1981, **52**, 7182.
42 S. Nosé and M. L. Klein, *Mol. Phys.*, 1983, **50**, 1055.
43 J. M. Míguez, M. M. Conde, J.-P. Torré, F. J. Blas, M. M. Piñeiro and C. Vega, *J. Chem. Phys.*, 2015, **142**, 124505.
44 U. Essmann, L. Perera, M. L. Berkowitz, T. Darden, H. Lee and L. G. Pedersen, *J. Chem. Phys.*, 1995, **103**, 8577.
45 W. L. Jorgensen, J. Chandrasekhar, J. Madura, R. W. Impey and M. Klein, *J. Chem. Phys.*, 1983, **79**, 926.
46 J. J. Potoff and J. I. Siepmann, *AIChE J.*, 2001, **47**, 1676.
47 J. S. Rowlinson and F. L. Swinton, *Liquids and Liquid Mixtures*, Butter-worths, London, 1982.
48 J. Costandy, V. K. Michalis, I. N. Tsimpanogiannis, A. K. Stubos and I. G. Economou, *J. Chem. Phys.*, 2015, **143**, 094506.

49 N. J. English and E. T. Clarke, *J. Chem. Phys.*, 2013, **139**, 094701.
50 B. J. Anderson, J. W. Tester and B. L. Trout, *J. Phys. Chem. B*, 2004, **108**, 18705–18715.
51 G. Pérez-Sánchez, D. González-Salgado, M. M. Piñeiro and C. Vega, *J. Chem. Phys.*, 2013, **138**, 084506.
52 P. D. Gorman, N. J. English and J. M. D. MacElroy, *Phys. Chem. Chem. Phys.*, 2011, **13**, 19780–19787.
53 J. S. Tse, M. L. Klein and I. R. McDonald, *J. Chem. Phys.*, 1984, **81**, 6146–6153.
54 S. Alavi, P. Dorman and T. K. Woo, *ChemPhysChem*, 2008, **9**, 911–919.
55 K. A. Udachin, C. I. Ratcliffe and J. A. Ripmeester, *J. Phys. Chem. B*, 2001, **105**, 4200–4204.
56 J. C. Platteeuw and J. H. van der Waals, *Mol. Phys.*, 1958, **1**, 91–96.
57 J. H. van der Waals and J. C. Platteeuw, *Adv. Chem. Phys.*, 1959, **2**, 1–57.
58 M. M. Conde, J.-P. Torré and C. Miqueu, *Phys. Chem. Chem. Phys.*, 2016, **18**, 10018–10027.